JOURNAL OF MATERIALS SCIENCE 19 (1984) 3515–3523

Degradation of Mn-doped $BaTiO_3$ ceramic under a high d.c. electric field

J. RÖDEL, G. TOMANDL*
Friedrick-Alexander-Universität, Erlangen-Nürnberg, Institut für Werkstoff Wissenschaften, Lehrstuhl III, Glas und Keramik, 8520 Erlangen Martensstrasse 5, West Germany

A manganese-doped $BaTiO_3$ was investigated with regard to the degradation of resistivity under a high d.c. electric field. Degradation was measured as a function of time, composition and temperature, using an electric field of 3 V μm^{-1}. The activation energy of the process was found to be 1.13 eV. to clarify the mechanism *I* against *U* characteristics and *I* against *T* graphs of new, degraded and relaxed samples were studied. Electron paramagnetic resonance and potential measurements were found to be useful in describing the degradation. Finally, a brief model is put forward to account for the observed phenomena. It is based on an injection of oxygen vacancies from the anode, which is accompanied by a reduction of manganese in the lattice.

1. Introduction

Barium titanate, because of its exceptionally high dielectric constant, has been used extensively as a capacitor material. A fatal characteristic, namely decreased insulation resistance (degradation) under high d.c. voltage stresses at high temperatures, has been observed, especially where recently developed acceptor-doped materials have been used. As the electric field in multi-layer capacitors is especially high, due to the very thin ceramic layers, these devices can be seriously affected by degradation.

There are several publications in this field, investigating single crystals [1, 2], polycrystalline $BaTiO_3$ [2–6] and multi-layer capacitors [7], as well as a very good review [8]. The interest of these workers, however, is often to measure the time of failure of tested specimens [4, 5, 7] and to perform accelerated life testing [5, 7]. The present authors' first interest was to record the time dependent degradation of four compositions as accurately as possible and find out whether there were various mechanisms leading to failure.

Several investigators into the degradation of $BaTiO_3$ [1–3, 6] have discussed a removal of oxygen ions from the lattice by reaction at the anode. This would result in the generation of anion vacancies, which might migrate to the cathode, pile up there and eventually facilitate the accurrence of Schottky emission. These suggestions were mainly based on potential measurements [1, 2] and absorption spectra [2, 9].

Oxygen concentration cell experiments indicated that ionic charge transport contributes appreciably to conductivity in these materials [3, 10]. If diffusion coefficients measured at high temperatures [11, 12] are extrapolated to temperatures around 200° C, however, it can be seen that the oxygen mobility is far too low to have any effect on the degradation mechanism. Furthermore, several workers state [13, 14] that below about 500° C $BaTiO_3$ ceramics cannot be reduced or reoxidized; oxygen ions are not mobile at all.

It was felt that the degradation mechanism was still very unclear. The present authors' second interest was thus to measure new, degraded and relaxed samples with regard to the *I* against *U* characteristics, the activation energy of conductivity and of degradation, and EPR resonances.

These results, together with a potential measure-

*Based on a thesis submitted by J. Rödel for the diploma degree at the Department of Ceramics, University of Erlangen, West Germany.

0022–2461/84 $03.00 + .12

ment, were performed to clarify the degradation process further.

2. Experimental details

2.1. Materials

Samples were sintered in either an oxidizing (air) or a reducing atmosphere (95% N_2, 5% H_2) at 1400° C for 200 min.* Samples were in the shape of disks or bars, the latter being, except for potential measurements, cut into flat disks. The compositions were as follows:

(I) $Ba_{100}Ti_{98}Mn_1O_{300-x}$

(II) $Ba_{100}Ti_{99}Mn_1O_{300-x}$

(III) $Ba_{100}Ti_{100}Mn_1O_{300+x}$

(IV) $Ba_{100}Ti_{101}Mn_1O_{300+x}$

Due to the great variation in the Ba/Ti ratio, the grain size varied from 2 to 100 μm and the density from 95.5 to 98.4%.

For all electric measurements except potential measurement, the sample thickness was 0.33 mm. Gold electrodes were sputtered on both sides. The electrode diameter was such as to leave a 1.5 mm ring of unelectroded ceramic at the edge to suppress arcing. The sample for potential measurement had a length of 13.3 mm and the front sides were completely electroded. New samples were used for each degradation run. For electron paramagnetic resonance (EPR) measurements specimens were ground to fine powder.

2.2 Change of resistance

The four compositions were tested as disks in air at 160° C. Samples were spring-loaded and held under an electric field of 3 V μm^{-1} for 250 h. At least five disks of each composition were measured.

For temperature-dependent measurements disks from bars of Composition I ($Ba_{100}Ti_{98}Mn_1O_{300-x}$) and four temperatures (160, 184, 202 and 226° C) were chosen. These experiments were conducted with three values of the electric field (0.50, 1.85 and 2.80 V μm^{-1}) to obtain more data and compare the results. The electric field was varied by various sample thicknesses at a constant applied voltage of 1 kV.

For measurements of the insulation resistance of the samples a computer-controlled apparatus was used. This recorded the electric current through the sample and calculated the resistance under consideration of the applied voltage. The apparatus was especially constructed for that purpose. The central unit is a logarithmic amplifier†, which can measure the electric current in a range from 10^{-10} to 10^{-3} A. Its output voltage is read by an analogue–digital converter†, which gives the data in the form of binary units to the computer. This decides whether the resistivity value has changed, and if so gives the order to store the new value on punch tape. This apparatus was set up to measure 20 samples in one run. Its accuracy is 10%. Two relays ensured that the degradation process was not interrupted while one switched. A resistor of 5 MΩ in series with each $BaTiO_3$ dielectric prohibited complete failure of the samples. As the resistance of the ceramic went down, the voltage drop occurred more and more over the built-in resistor of 5 MΩ. Thus the electric field in the $BaTiO_3$ dielectric was lowered. This allowed further investigation of the degraded samples.

2.3. Relaxation and annealing

Samples were termed relaxed when the voltage was switched off after degradation and they were kept for 40 h in the short-circuited state. After degradation a few of the samples were annealed by heating them to around 500° C and holding them there for 1 h. They were then taken out of the furnace. The electrodes had been removed previously by careful grinding.

2.4. I against U characteristics

Measurements were performed for all compositions with new, degraded and relaxed samples. It was ensured that degraded samples could not relax and samples did not degrade. Recordings of the electric current were taken with the apparatus described above. All characteristics were reproducible and taken for at least five samples.

2.5. Activation energy of conductivity

The dependence of the conductivity of the samples on temperature was measured before and after degradation. Disks from a bar of Composition I ($Ba_{100}Ti_{98}Mn_1O_{300-x}$) were chosen. During the

*Samples kindly supplied by R. Wernicke, Philips Research Laboratory, Aachen.
†Function Modules, Inc.

degradation process at 235° C under an electric field of 2.00 V μm^{-1} the resistance of the samples decreased by more than two orders of magnitude. The electric current in the range from 133° C to 235° C was recorded under an electric field of 0.37 V μm^{-1} with the apparatus described above.

2.6. Electron paramagnetic resonance

An X-band paramagnetic spectrometer (9.5 GHz) with 100 kHz field modulation was used. All measurements were performed at room temperature.

2.7. Potential measurement

A bar of Composition I ($Ba_{100}Ti_{98}Mn_1O_{300-x}$) was turned to give a cylinder with a diameter of 5 mm and a length of 13.3 mm. Five small grooves were mill-cut round the sample along its length. Platinum wires were positioned in these and connected to high voltage relays. The relays were controlled by a small voltage which in turn was controlled by hand. The potential at these five positions was alternatively measured with an electrometer with "infinite" internal resistance. The sample was situated in a silicone oil bath at 226° C. The voltage applied was 6.1 kV. In this case no resistor in series was built in, but the applied voltage was switched off when a certain current was reached. Potential and resistance could thus be measured independently without the slightest interruption during the experiment.

3. Results

3.1. Change of resistance

Two types of degradation behaviour were observed (Fig. 1). The first type, which is represented by all our disk-shaped samples sintered in air and tested under standard conditions (3 V μm^{-1}, 250 h, 160° C), can be described by a straight line in Fig. 1. This represents a steady decrease of resistivity with time.

The equation then is:

$$R = R_1\left(\frac{t}{t_1}\right)^{-m} \qquad m > 0, \qquad (1)$$

where R, R_1 are resistances after some time t, t_1 respectively; m varies from 0.1 (Composition II) to 1.1 (Composition I), but differs little among samples of the same composition.

The second type of degradation is only represented by Composition II, the stoichiometric composition, if sintered under reducing atmospheres, or, if sintered in air, tested under a higher d.c. electric field for 300 h. The latter case was chosen for Fig. 1. This behaviour can be approximated by two straight lines in Fig. 1 or two equations like Equation 1, which are valuable in different sections and have different slopes m and reference times t_1, t_2. The time corresponding to the cross-over of the two lines is termed here the characteristic lifetime. The decrease of resistance up until this time is usually little, but from then on is very rapid. However, it is not a sudden breakthrought, but – as in the case shown here – lasts 30 h.

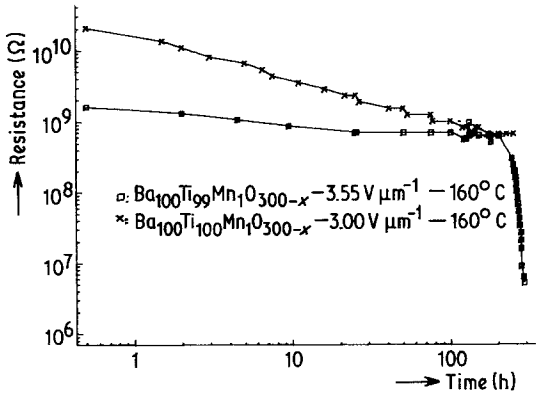

Figure 1 First and second type of degradation behaviour.

Some results for samples sintered in air are shown in Fig. 2. Here the ratio of resistance before and after degradation is given. The barium-rich Composition I, which is the one with the lowest density and the one which sinters badly, shows the greatest scatter. Composition IV is shown with data measured and extrapolated. The latter were gained under the assumption, that the built-in

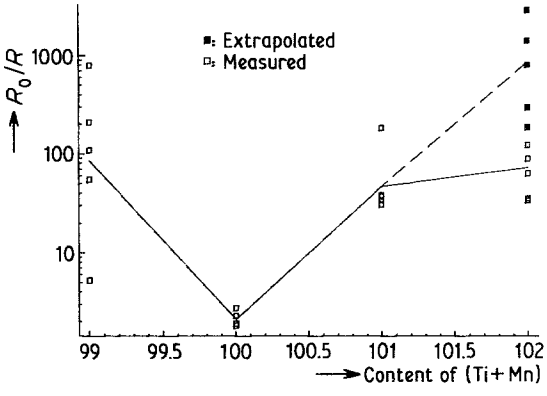

Figure 2 Ratio of original resistance to resistance after standard degradation experiment as a function of Mn + Ti.

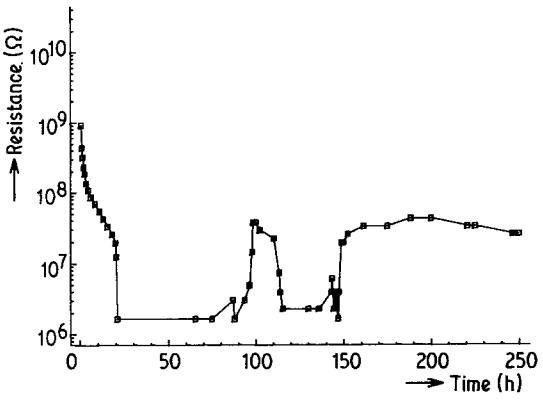

Figure 3 Typical example of relaxation and renewed degradation during the experiment.

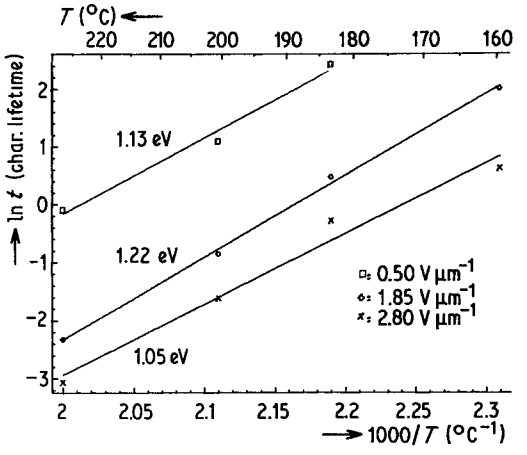

Figure 4 Characteristic lifetime as a function of reciprocal temperature.

resistor for limiting degradation is taken out, so that degradation is not stopped at a certain level (which happened only in this case). The good result for Composition II is misleading, It is expected that its resistance would drop after some longer experimental time. This also means that a comparison of data as shown in Fig. 2 is very suspect and a detailed investigation of mechanisms involved is necessary.

First, however, a very special degradation behaviour presented in Fig. 3 will be examined. This sample degrades very quickly and under the effect of the built-in resistor the electric field on the sample is lowered. This allows it to relax, the resistance increases again and renewed degradation occurs. This, however, is not typical for all samples of that composition.

Further results for disks sintered in reducing atmospheres will not be discussed now, because compositions with high titanium-content had such a low resistance that they could not be degraded at all with our apparatus and samples with high barium-content showed little change of resistance with time under standard test conditions for times up to 600 h.

3.2. Activation energy of degradation

Previous investigators into the degradation of ceramic capacitors used various criterions to define failure and lifetime of tested samples [4–7]. It was decided to look for a reproducible material which show degradation of the second type and to plot characteristic lifetime against the reciprocal of temperature.

Bars of Composition I, in contrast to disks of the same composition, showed the required type of degradation. This discrepancy between the sintered body was ascribed to a higher density and a greater homogeneity of the bars in comparison to the disks.

The activation energy of degradation, which was gained from three series of measurements (Fig. 4), was calculated to be 1.13 ± 0.1 eV. This is in excellent agreement with results from Minford [7], who measured multilayer ceramic capacitors with high dielectric constant ϵ and obtained 1.19 ± 0.05 eV. Prokapwicz and Vaskas [15], however, reported a lower value (0.90 eV) for a capacitor with medium ϵ.

3.3. Relaxation and annealing

Relaxation of degraded samples was already mentioned in [6] and [8]. It was noticed that there was an increase of resistance by a factor of 1.5 to 4 through this mechanism. Renewed degradation was recorded and compared with the degradation of a sample for which the polarity was reversed after testing (Fig. 5). It can be clearly seen that the sample returns quickly to its degraded value in the first case, but does so rather slowly in the second case.

The effect of annealing is also well known [16]. Only a few experiments were performed and it was observed that a complete healing of samples was achieved by heating them to 520° C and an incomplete healing by heating them to temperatures lower than 500° C. The term healing is used to describe the fact that a sample takes up its original resistance as before the test. It was not the intention to measure that quantitatively, but

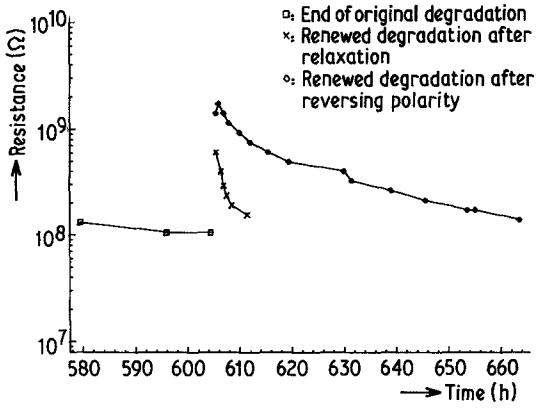

Figure 5 Renewed degradation of a relaxed sample and of a sample with reversed polarity.

merely to check it, as it is an important argument for discussion.

3.4. *I* against *U* characteristics

Little is known about *I* against *U* characteristics of degraded samples [2] and nothing is known about these experiments for relaxed samples. The present measurements could be clearly related to the two types of degradation descibed above. Correspondingly, various *I* against *U* characteristics can be termed either first type or second type (Fig. 6).

3.4.1. First type

This is represented by a measurement of the sample, the degradation of which was described before in Fig. 1 (Composition III). The lower curve shows the characteristic of the new sample which is almost ohmic. The upper curve represents the degraded ceramic. It can be seen that up to 50 V its characteristic is ohmic as well, but then the curve gets steeper and finally has a slope s of 2.4 (Equation 2):

$$I \propto V^s. \tag{2}$$

The behaviour of a relaxed sample lies just in between a new and degraded ceramic.

At present it is suggested that the first type of degradation creates an increased number of charge carriers. the mobility of which is limited at low voltages by space charges.

3.4.2. Second type

This is represented here by a sample of Composition II sintered in reducing atmosphere. The resistance of the ceramic decreased by more than two orders of magnitude during the degradation process and remained stable till the end of experiment. This time of constant resistance is considered to be long enough to level out internal electric charges. Thus the *I* against *U* characteristics of new, relaxed and degraded samples are about parallel. The difference in height represents the different conductivity in the various states.

There was a proposal by Payne [3], to relate the *I* against *U* characteristics of materials to their reliability in life tests. A relationship like that could not be found and it is estimated and in view of the complex dependences of degradation on electric field, temperature and composition, that this is an uncertain and difficult approach to make predictions.

3.5. Activation energy of conductivity

The results are shown in Fig. 7. There is a definite difference in the activation energy of samples before and after degradation, which is 1.0 eV and

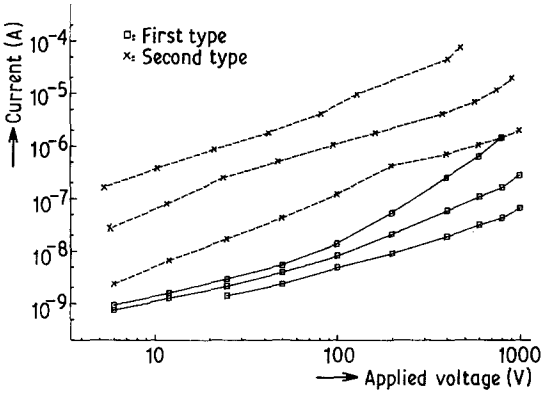

Figure 6 First and second type of *I* against *U* characteristics.

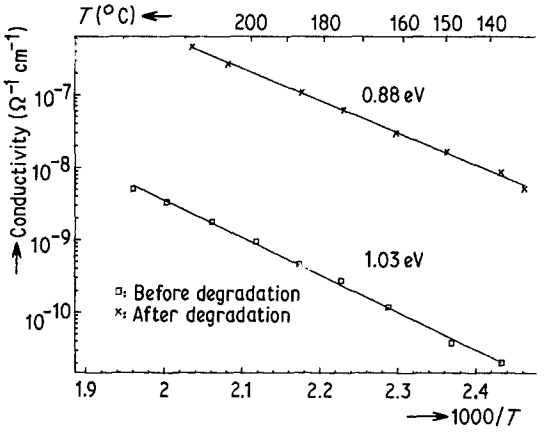

Figure 7 Conductivity before and after degradation as a function of reciprocal temperature.

0.88 eV, respectively. This can be correlated to Hagemann's measurements [17] of the activation energy of a manganese-doped $BaTiO_3$ ceramic. He found 1.0 eV for samples annealed in air or nitrogen and 0.8 eV for samples annealed in a reducing (using H_2) atmosphere. Hagemann suggested that these activation energies are related to the energy levels of Mn^{2+} and Mn^{3+} in the forbidden energy gap. This is in contradiction to [6], where an activation energy of 0.4 eV for low temperatures and of 1.0 eV for higher temperatures for a degraded sample (a.c. degradation) was reported.

3.6. Electron paramagnetic resonance

There is an excellent correspondence between all the present measurements. The effect of degradation can be clearly seen in EPR spectra, the better the greater the decrease in resistance is and independent of the type of degradation. The results are summarized in Fig. 8.

The lowest resonance shows a disk from a bar of Composition I ($Ba_{100}Ti_{98}Mn_1O_{300-x}$), degraded at 235° C under an electric field of 2.00 V μm^{-1} with a change of resistance of three orders of magnitude. The other spectra show a disk from the same bar, where degradation was performed at the same temperature under field of 0.63 V μm^{-1}. The experiment was stopped when the resistance of the latter sample dropped to 5% of its initial value. Thin disks (150 μm) of the 2 mm thick ceramic were cut off near cathode and anode. These were also ground and measured by EPR.

In comparing the spectra of the new sample with the degraded ceramic a multiplet can be seen developing in the latter. It is suggested that this resonnance is due to the hyperfine splitting: it originates from the interaction between the electrons of Mn^{2+} ($3d^5$) and the Mn^{55} nucleus of spin $I = 5/2$. The g-factor of these multiplets could not be measured very accurately, but our value of $g = 2.009 \pm 0.01$ is in agreement with literature data for Mn^{2+}, which give a value of $g = 2.002$ [18, 19]. Furthermore, the present measurement of hyperfine constant $A = 85 \pm 1$ G is in good correspondence to [18], where $A = 85$ G and [19], where $A = 84$ G was found.

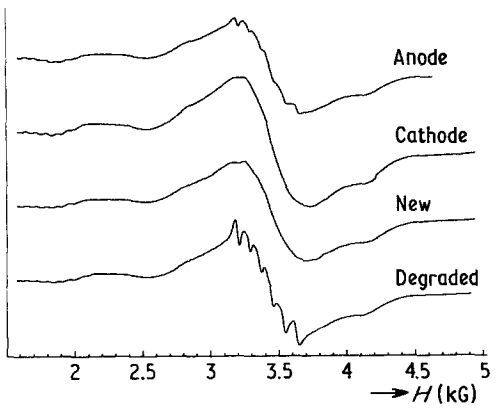

Figure 8 Electron paramagnetic resonance of new and degraded samples.

That this multiplet is due to Mn^{4+} can also be discarded, as the corresponding data in the literature [18] are $g = 1.994$ and $A = 75$ G. Also, spectra of Mn^{4+} in $BaTiO_3$ cannot be seen at room temperature [14, 20]. As manganese in $BaTiO_3$ ceramics sintered in air occurs either as Mn^{3+} or Mn^{4+} [14], the Mn^{2+} must have been formed by the degradation process. The resonance of the materials near anode and cathode clearly shows that this mechanism starts at the anode.

3.7. Potential measurement

Only the potential measurement of a sample with the second type of degradation can be presented here. The dependence of resistance on time is shown in Fig. 9a. Corresponding potential curves can be seen in Fig. 9b. A local resistivity (Fig. 9c) was calculated using Equation 3:

$$\rho_{\text{loc.}} = \frac{E_{\text{loc.}}}{j}. \tag{3}$$

The local electric field needed for Equation 3 was obtained by graphical differentiation of Fig. 9b. Fig. 9c thus requires interpretation with caution. Some important observations can be made however; A field of a relatively high potential drop or local resistance is built up at the anode soon after the beginning of the experiment. This moves slowly to the cathode. This high potential drop seems to increase slightly in size while it is moving and corresponds to a local field, which is about double the size (1.0 V μm^{-1}) of the overall electric field (0.47 V μm^{-1}). When it arrives at the cathode, the resistance of the sample starts to decrease. Before this, it even shows a small increase, due to that inner field of a high local resistance.

During the experiment the local resistance near the anode decreases steadily while it first remained constant at the cathode (this is not the case with No. 3, but a change of potential by 0.1 kV, which

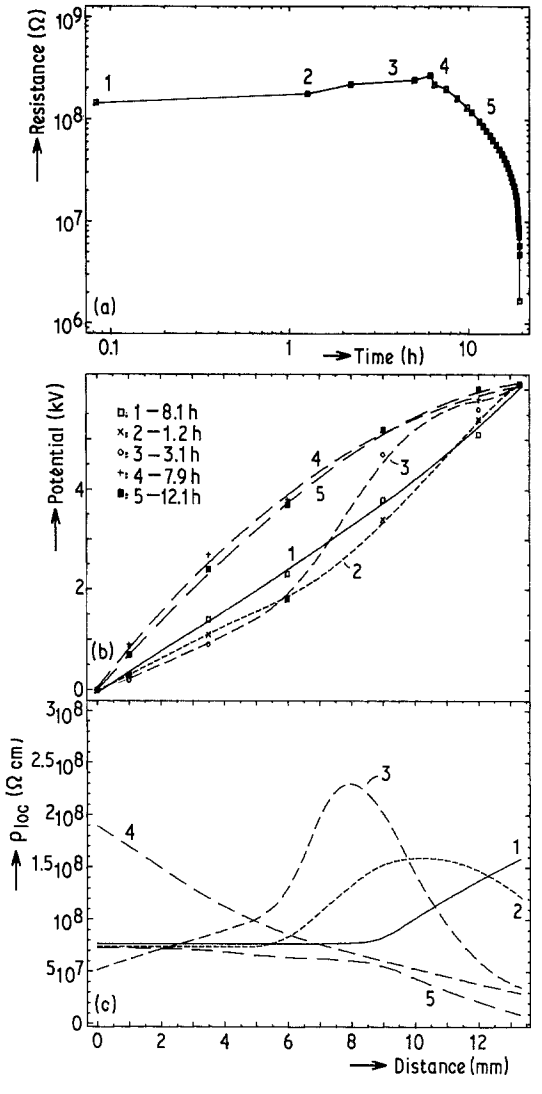

Figure 9 (a) Resistance against time of treatment for potential measurement. (b) Potential distribution. (c) Local resistivity.

is in the range of error probability, would give the same value as Nos. 1 and 2).

When this certain frontier arrives at the cathode the local electric field at the anode is already as low as 0.1 V μm^{-1}.

The local resistance further decreases near the anode and also does so near the cathode, where the maximum remains. Thus the overall conductivity of the sample increases more and more until this finally leads to Joule heating and thermal breakdown.

These results correspond well with comparable measurements by Goto and Kachi [1] and Lehovec and Shirn [2]. These investigators, however, could not observe a degradation with a final breakthrough and/or could not record the resistance against time as defined as we could.

4. Discussion

Although there are still some details open to question, the authors now feel in the position to present a further advanced model, which accounts for the degradation mechanism. First the materials which show degradation of the second type will be discussed and later the difference of behaviour of the first type will be mentioned.

EPR measurements revealed, that an increasing amount of Mn^{2+} is created from Mn^{3+} or Mn^{4+} during the degradation process. This seems to occur close to the anode rather than near the cathode. It is thought that this is not due to a negative space charge in the material where additional electrons are located at the energy levels of the acceptor dopant, and so a redox mechanism must be considered. While manganese is reduced according to Equation 4,

$$Mn^{4+} + 2e^- \rightarrow Mn^{2+}, \quad (4)$$

it is most probable that oxygen in the lattice is oxidized. This means that oxygen ions have to move to the anode and, either by oxidation of electrode material or evaporation according to Equation 5,

$$O^{2-} \rightarrow 2e^- + 1/2\,O_2, \quad (5)$$

leave the lattice and give two electrons to the anode. This might be also expressed as an oxygen vacancy injection from the anode. It is suggested that the diffusion of oxygen ions to the anode is the first step. The second step is the injection of oxygen vacancies, which move forward and consecutively create a positive space charge, which as a third step is balanced by conducting electrons trapped at the manganese lattice sites. Oxygen vacancies are thus taking part in the charge transport. This mechanism might also be termed an electric field-assisted one-way diffusion. It occurs preferentially at high electric fields and high temperatures. Its measured activation energy (1.13 eV) is in a range which might be conceivable for the diffusion of oxygen vacancies. These play the crucial part in the degradation process and not – as might be possible – migrating cations, which was checked by X-ray fluorescense analysis.

Before going into further detail, however, the conduction mechanism in acceptor-doped polycrystalline $BaTiO_3$ should be reconsidered.

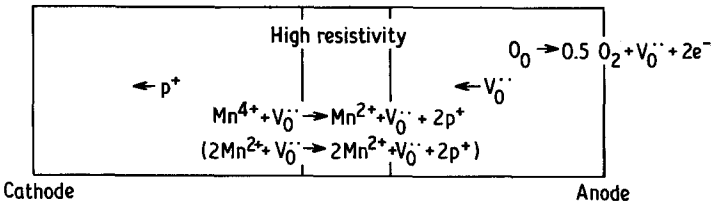

Figure 10 Schematic description of degradation process.

Both the conductivity mechanism and the defect chemistry in this material at temperatures higher than 500° C are best described by Hagemann [14]. At high partial pressures of oxygen p-type conductivity dominates: around a p_{O_2} of 10^{-10} the conductivity is a minimum and changes to n-type at lower partial pressures. It should be borne in mind that this model is much simplified and only partly accounts for the situation in the temperature range used. Still it is possible to make some points, where an attempt will be made to correlate the potential measurement and possible conduction mechanism.

Degradation has been considered as a quasi-reduction process. A slightly reduced Mn-doped $BaTiO_3$, however, has a higher insulation resistance to one tempered in air [21]. That is reasonable if we consider the injection of oxygen vacancies. Under the influence of the electric field these will move towards the cathode and will be captured most probably at a manganese lattice site, where charge neutralization can occur easily. Then electrons at these sites must be activated from a Mn^{2+}–$V_0^{\cdot\cdot}$ complex, which might well be more difficult compared to a Mn^{3+} level. It it thus suggested that the front of a high local resistance observed in potential measurement can be ascribed to this Mn^{2+}–$V_0^{\cdot\cdot}$ complex. The decreasing local resistance might then be due to a further increasing number of oxygen vacancies in the $BaTiO_3$, which in turn will effect a further reduction of Mn^{2+} to Mn^{1+}. This mechanism goes on and leads to a further decreasing local resistance near the anode. These simple reactions are briefly summarized in Fig. 10.

As it cannot be supposed that electron injection plays an important part in the beginning of the degradation process, it is reasonable, that the local resistivity near the cathode remains constant until the front of a high electric field arrives there. Now the mechanism of the actual breakdown still needs to be clarified:

As stated above, it is assumed that the moving front of oxygen vacancies effects a positive space charge. When this arrives at the cathode the work function of the electrode material is lowered (Schottky emission) and the positive space charge, which might otherwise tend to slow down the process, is more easily neutralized at the cathode than inside the material. The quasi-reduction process is thus accelerated. Oxygen vacancies still move towards the cathode, the overall conductivity is further increasing, Joule heating occurs and will lead finally to thermal breakdown.

As it has been assumed that electronic carriers, which dominate the charge transport, are activated from different energy levels before and after degradation, it is reasonable, that the activation energy changes during the process, the Fermi level is shifted to higher values. The I against U characteristic of samples of the second type confirms this result. A degraded sample with limited decrease of resistivity shows predominantly ohmic behaviour, but an increase of electronic carriers.

If the annealing procedure is examined further confirmation is found that a change in the oxygen defect chemistry plays a vital part in the degradation process. At temperatures high enough to enable equilibration with the surrounding atmosphere by diffusion of oxygen ions, samples can regain their original resistance. At last the relaxation mechanism points to zones or spikes [2], along which the degradation occurs favourably. These might be grain boundaries, which would correspond with experiments from [2], but contradict with results from [11], or inhomogeneities. Along these paths oxygen vacancies would predominantly move and build up space charges. While samples relax, charge equilibration between zones or spikes and bulk through electronic carriers might be possible; conducting paths might fade away. This argument would also account for the special type of renewed degradation encountered in Fig. 3.

Finally, it is assumed that the first type of degradation is a process where the material has a high inhomogeneity. It is supposed that space charges are more important and degradation

fronts proceed more or less fast along the various paths. Still, this would not account for the rather well defined degradation curves which have been measured. It is felt that the process is more complicated in this case and further investigations must be carried out before a more detailed discussion can be reopened.

5. Conclusions

In the present model it is suggested that an electric field assisted one-way diffusion of oxygen vacancies plays the crucial part in the degradation process. Oxygen ions thus contribute little to the conduction mechanism, but manage to change it.

The assumption of a quasi-reduction along favourable paths in the test material allows an explanation of the measurements and relates them to the results of other investigators.

There are various details still open to question, but it is hoped that a contribution has been made to a further advanced understanding. More detailed experiments, taking into account various microstructures and various acceptor dopants as well as a further investigation into various types of degradation, would give valuable results.

Acknowledgements

The authors would like to thank R. Wernicke, H. J. Hagemann and D. Hennings from the Philips Research Laboratory, Aachen, for their valuable help in sample preparation, literature review and discussion.

References

1. Y. GOTO and S. KACHI, *J. Phys. Chem. Sol.* **32** (1971) 889.
2. K. LEHOVEC and G. A. SHIRN, *J. Appl. Phys.* **33** (1962) 889.
3. D. A. PAYNE, Proceedings of the Sixth Annual Reliability Physics Symposium, IEEE, California (New York, 1968) p. 257.
4. J. B. MACCHESNEY, P. K. GALLAGHER and F. V. DIMARCELLO, *J. Amer. Ceram. Soc.* **46** (1963) 197.
5. K. OKAZAKI and H. IGARASKI, *Ferroelectrics* **27** (1979) 263.
6. W. A. SCHULZE, L. E. CROSS and W. R. BUESSEM, *J. Amer. Ceram. Soc.*, **63** (1980) 83.
7. W. J. MINFORD, *IEEE Trans. Components, Hybrids, Manuf. Technol.*, **5** (1982) 297.
8. R. M. GRUVER, W. R. BUESSEM, C. W. DICKEY and J. W. ANDERSON, *Tech. Rept. AFML-TR-66-164* (1966) 223.
9. V. Ya. KUNIN, A. N. TSIKIN and N. A. SHTURBINA, *Sov. Phys. Solid State* **11** (1968) 598.
10. D. D. GLOWER and R. C. HECKMAN, *J. Chem. Phys.* **41** (1964) 877.
11. C. SCHAFFRIN, *Phys. Status Solidi (a)* **35** (1976) 79.
12. R. WERNICKE, *Philips Res. Rep.* **31** (1976) 526.
13. T. TAKEDA and A. WATANABE, *J. Phys. Soc. Jpn.* **21** (1966) 267.
14. H. J. HAGEMANN, Ph.D. Thesis, RWTH Aachen (1980).
15. T. I. PROKOPOWICZ and A. R. VASKAS, Final Rep., ECOM–90705–F (1969); MTIS AD-864068.
16. L. BENGUIGUI, *J. Phys. Chem. Solids* **34** (1973) 573.
17. H. J. HAGEMANN, *Ber. Dt. Keram. Ges.* **55** (1978) 353.
18. J. B. DESU and E. C. SUBBARAO, "Advances in Ceramics", Vol. I, edited by L. M. Levinson (American Ceramic Society, Ohio, 1981) p. 189.
19. H. IKUSHIMA and S. HAYAKAWA, *J. Phys. Soc. Jpn.* **19** (1964) 1986.
20. M. NAKAHARA and T. MURAKAMI, *J. Appl. Phys.* **45** (1974) 3795.
21. R. WERNICKE, Personal communication.

Received 24 December 1983
and accepted 18 January 1984